

ANALYSIS OF CONTRACTIONS IN SYSTEM GRAPHS: APPLICATION TO STATE ESTIMATION

Mohammadreza Doostmohammadian^{†*}, Themistoklis Charalambous[†], Senior Member, IEEE,
Miadreza Shafie-khah^{*}, Hamid R. Rabiee[◊], Senior Member, IEEE,
and Usman A. Khan[‡], Senior Member, IEEE

[†] School of Electrical Engineering, Aalto University, Espoo, Finland.

^{*} Faculty of Mechanical Engineering, Semnan University, Semnan, Iran.

^{*} School of Technology and Innovations, University of Vaasa, Vaasa, Finland

[◊] Computer Engineering Department, Sharif University of Technology, Tehran, Iran

[‡] Electrical and Computer Engineering Department, Tufts University, Medford, MA, USA.

ABSTRACT

Observability and estimation are closely tied to the system structure, which can be visualized as a *system graph*—a graph that captures the inter-dependencies within the state variables. For example, in social system graphs such inter-dependencies represent the social interactions of different individuals. It was recently shown that contractions, a key concept from graph theory, in the system graph are critical to system observability, as (at least) one state measurement in every contraction is necessary for observability. Thus, the size and number of contractions are critical in recovering for loss of observability. In this paper, the correlation between the average-size/number of contractions and the global clustering coefficient (GCC) of the system graph is studied. Our empirical results show that estimating systems with high GCC requires fewer measurements, and in case of measurement failure, there are fewer possible options to find substitute measurement that recovers the system’s observability. This is significant as by tuning the GCC, we can improve the observability properties of large-scale engineered networks, such as social networks and smart grid.

Index Terms— Contraction, clustering coefficient, structural observability, estimation, system graph

1. INTRODUCTION

Large-scale networked systems have seen a surge of interest in recent control and signal processing literature with applications in IoT and CPS [1–3]. A key challenge in such networks is state estimation [2, 4, 5] via a distributed network of measurements. From this perspective of distributed estimation,

an effective tool is the system graph in which nodes represent state variables and edges between two nodes show coupling among the two state variables [6–8], motivating structural control and graph signal processing. In this sense, structural observability is related to certain system graph properties relying only on the system structure, and not on the exact system parameter values [4, 6, 7, 9].

An important graph-theoretic property to study system observability is the notion of *contraction* in the system graph, which is the dual of *dilation* in controllability [7]. In a contraction, multiple nodes are contracted (connected) to a fewer group of nodes. It is known that measuring one state node in every contraction is essential for network observability [10, 11]. All states in a contraction are thus observationally equivalent which is significant for observability recovery, for example, in sensor/measurement failure [4, 11]. The size of contractions is also a key property, representing the number of possible options for estimation/observability recovery. A large contraction presents more choices of equivalent state measurements to replace the failed/faulty observation, or, for example, to minimize cost [12–14]. Also, the number of contractions represents the number of necessary measurement (or sensors) for estimation. The size and distribution of contractions in a system graph depend on certain graph properties. This work particularly studies how the *global clustering coefficient* affects the distribution of contractions. This paper is a nonlinear model extension of our previous works [1, 10] on *local clustering coefficient* and *degree heterogeneity*.

This paper models the nonlinear system as a random Scale-Free (SF) graph. The reason is that the structure of most real-world systems resemble the structure of SF graphs [15]. To study the effect of the GCC, as our main contribution, the distribution of size/number of contractions in SF graphs and clustered SF (CSF) graphs are compared. Due to specific formation in CSF graphs (known as *triad formation*) they have higher GCC, while their other properties (particularly

This work is partially supported by National Science Foundation under awards #1903972 and #1935555. Corresponding author email: doost@semnan.ac.ir, mohammadreza.doostmohammadian@aalto.fi

power-law degree distribution) are similar to SF graphs. The significance of this contribution is that by tuning the network GCC, e.g., adopting the results of [16, 17], one can improve/impair system observability properties. Our results can be used in the design of large-scale man-made networks to improve their estimation properties in terms of reducing necessary observer nodes (sensor locations) for cost-optimal estimation. An example of such re-design of power grid is given in Section 5 as another contribution of this paper. Another possible application is in changing the structure of social networks to hinder the possibility of distributed estimation [18, 19] and, therefore, improve information privacy and reduce the vulnerability towards information leakage [20].

The rest of this paper is as follows. Section 2 describes graph-theory notions to define the contractions. Section 3 states the specific application to system estimation and observability. In Section 4, the distribution of contractions in SF and CSF graphs are compared, and an illustrative example application in power grid monitoring is given in Section 5. Conclusions and future research are presented in Section 6.

2. CONTRACTIONS IN GRAPHS

We consider the complex system, for example a social system, as an undirected graph or a strongly-connected directed graph (SC digraph) denoted by $\mathcal{G} = (\mathcal{V}, \mathcal{E})$, with the node set \mathcal{V} (representing the n states) and edge/link set $\mathcal{E} = \{(v_i, v_j)\}$. The associated bipartite system graph $\Gamma = (\mathcal{V}^+, \mathcal{V}^-, \mathcal{E}_\Gamma)$ is defined with two disjoint left/right node sets \mathcal{V}^+ and \mathcal{V}^- , and edges $\mathcal{E}_\Gamma = \{(v_j^-, v_i^+) | (v_j, v_i) \in \mathcal{E}\}$. In \mathcal{G} , the edges with no common end node are called a matching $\underline{\mathcal{M}}$, which equivalently in Γ represent the subset of edges not incident on the same node in \mathcal{V}^+ . In other words, $\underline{\mathcal{M}}$ is a set of pairwise disjoint edges (with no loop). A matching with maximum size is called maximum (cardinality) matching \mathcal{M} , which is not a subset of any other matching. Note that there are many possible choices of \mathcal{M} in general. The nodes respectively in \mathcal{V}^+ and \mathcal{V}^- incident to the chosen \mathcal{M} are denoted by $\partial\mathcal{M}^+$ and $\partial\mathcal{M}^-$, and the nodes in $\delta\mathcal{M} = \mathcal{V}^+ \setminus \partial\mathcal{M}^+$ are unmatched in \mathcal{V}^+ . Given \mathcal{M} , let $\Gamma^{\mathcal{M}}$ be the auxiliary graph made by reversing all edges in \mathcal{M} , and holding all the other edges $\mathcal{E}_\Gamma \setminus \mathcal{M}$ in Γ . In $\Gamma^{\mathcal{M}}$, an alternating path associated to \mathcal{M} (also called \mathcal{M} -alternating path), denoted by $\mathcal{Q}_\mathcal{M}$, is a path starting from a node in $\delta\mathcal{M}$ with its edges alternately in \mathcal{M} and not in \mathcal{M} . An augmenting path $\mathcal{P}_\mathcal{M}$ associated to \mathcal{M} (also called \mathcal{M} -augmenting path) is an \mathcal{M} -alternating path in $\Gamma^{\mathcal{M}}$ that starts from and ends in $\delta\mathcal{M}$. For a matching $\underline{\mathcal{M}}$ and associated $\mathcal{P}_\mathcal{M}$, $\underline{\mathcal{M}} \oplus \mathcal{P}_\mathcal{M}$ represents a new matching with one more edge than $\underline{\mathcal{M}}$, where \oplus is the XOR operator. In $\Gamma^{\mathcal{M}}$, a contraction \mathcal{C}_j , associated to an unmatched node $v_j \in \delta\mathcal{M}$, is defined as the set of all state nodes in \mathcal{V}^+ reachable by \mathcal{M} -alternating paths starting from v_j . Intuitively speaking, contraction represents subset of nodes linking to smaller subset of nodes [10,21]. Algorithm 1 [10,21] presents the pseudo-code for finding graph contractions with polynomial order com-

plexity $\mathcal{O}(n^{2.5})$. Polynomial complexity facilitates applications in large-scale as in social networks or power grids.

Algorithm 1: Finding contractions in a graph [10,21].

Given: System graph \mathcal{G}
 Find Γ ;
 Find $\underline{\mathcal{M}}$;
 Find $\Gamma^{\underline{\mathcal{M}}}$;
while $\mathcal{P}_\mathcal{M}$ exist **do**
 for nodes in $\delta\mathcal{M}$ **do**
 Find $\mathcal{P}_\mathcal{M}$;
 $\underline{\mathcal{M}} = \underline{\mathcal{M}} \oplus \mathcal{P}_\mathcal{M}$;
 Find $\Gamma^{\mathcal{M}}$;
for state nodes in $\delta\mathcal{M}$ **do**
 Find $\mathcal{Q}_\mathcal{M}$ in $\Gamma^{\mathcal{M}}$;
 Put nodes in \mathcal{V}^+ reachable by $\mathcal{Q}_\mathcal{M}$ in \mathcal{C}_i ;
Return $\mathcal{C}_i, i = \{1, \dots, l\}$;

In this paper, as our main contribution, we aim to understand possible correlation between the GCC and prevalence of contractions, and interpret the implication of this relation through a system estimation perspective.

3. APPLICATION TO STATE ESTIMATION

In this work, a *nonlinear* autonomous dynamic system (in contrast to the linear model in [10]) is considered as,

$$\dot{\mathbf{x}} = f(\mathbf{x}(t)) + \mathbf{v}, \quad (1)$$

where the state variable $\mathbf{x} = [x^1, \dots, x^n]^\top \in \mathbb{R}^n$ is to be estimated via the measurements,

$$\mathbf{y}(t) = g(\mathbf{x}(t)) + \mathbf{r}, \quad (2)$$

where $\mathbf{y} = [y^1, \dots, y^m] \in \mathbb{R}^m$ is the measurement, and \mathbf{v} and \mathbf{r} are Gaussian noise. The system model (1)-(2) can be represented as a Linear-Structure-Invariant (LSI) model as,

$$\dot{\mathbf{x}} = A(t)\mathbf{x}(t) + \mathbf{v}, \quad (3)$$

$$\mathbf{y}(t) = C(t)\mathbf{x}(t) + \mathbf{r}, \quad (4)$$

where $A(t)$ and $C(t)$ are time-dependent system and measurement matrices representing the linearization of the system and measurement functions $f(\cdot)$ and $g(\cdot)$ over time. Recall that, from Kalman filtering theory, the underlying system can be estimated if it is *observable* via the given measurements. System observability implies that the global vector, \mathbf{x} , can be uniquely determined by the measurements, \mathbf{y} . As shown in [7], the observability of the nonlinear model (1)-(2) is equivalent with the observability of the linearized model (3)-(4) over all operating points. The structure (the zero-nonzero pattern) of the associated linearized matrices

$A(t)$ and $C(t)$ are time-invariant while the numerical values of their nonzero entries may vary at different operating points, implying the name structure-invariant. This motivates the concept of *structural observability* (or *generic observability*) based on structured systems theory [6, 7, 9], which provides a graph-theoretic method to check for system observability. In structural analysis the system is modeled as a *system graph*, where a node v_i models a state x^i and a link $v_j \rightarrow v_i$ models the dependency of the two state variables x^i and x^j . In other words, if f^i is a function of x^j then the entry $\frac{\partial f^i}{\partial x^j}$ in linearized matrix A is nonzero while its exact value depends on the operating point and may change over time [9, 19]. Denote the system graph by $\mathcal{G}_A = (\mathcal{V}, \mathcal{E}_A)$, with state nodes \mathcal{V} and $\mathcal{E}_A = \{(v_j, v_i) \mid \frac{\partial f^i}{\partial x^j} \neq 0\}$ including the edges $v_j \rightarrow v_i$. Using the definitions in Section 2, the next theorem states necessary conditions for observability of the system graph \mathcal{G}_A .

Theorem 1 *Let $\delta\mathcal{M}$ denote the set of unmatched nodes of system graph \mathcal{G}_A associated with an autonomous LSI system. To ensure observability, it is necessary to measure every unmatched state in $\delta\mathcal{M}$.*

We refer to [7] for the proof (in the dual case of controllability). Based on the definition, for a given maximum matching \mathcal{M} , every node $v_j \in \delta\mathcal{M}$ belongs to a contraction \mathcal{C}_i , while the nodes $\mathcal{C}_i \setminus v_j$ are all matched. This leads to the following *observational equivalence* property in contractions:

Theorem 2 *Consider an LSI system abstracted as a graph (undirected or SC) with contractions $\mathcal{C} = \{\mathcal{C}_1, \dots, \mathcal{C}_m\}$. The necessary condition for observability is to measure (at least) one state node in every contraction.*

Corollary 1 *Nodes in a contraction are equivalent for observability recovery.*

See the proofs in [10, 11]. This corollary implies that when a critical measurement fails, causing loss of observability, measurement of any other state node in the same contraction recovers the system observability [4]. Recall that (structural) rank deficiency of the system matrix A defines the cardinality of $\delta\mathcal{M}$ and \mathcal{C} in its associated system graph \mathcal{G}_A [21, 22].

4. CONTRACTION PREVALENCE IN SF GRAPHS

In this section, the distribution of contractions in SF networks, as random graph-representations of real-world systems, is studied. Such random models simplify the understanding of different processes, e.g., spreading processes and cascading failures [15, 23–25]. The main feature of SF graphs is their *power-law degree distribution* [15], which implies that there are few hubs (nodes with high degree) and large number of low-degree nodes in the SF network. To construct such networks, Ref. [15] provides an iterative algorithm initializing with a small *seed graph* and recursively adding a new node

with m new edges. The main feature of this iterative procedure is that the linking probability between the new node and an old node is proportional to its degree. In other words, the new node *prefers* connecting to old hubs, hence it is named *preferential attachment*. Such SF graphs are known to have low GCC¹, while real-world networks, for example social networks, show high clustering. Therefore, a modified model with high GCC is proposed [23–25], named Clustered Scale Free (CSF). The building blocks of this model are similar to the preferential attachment, where the difference is the *triad formation* step. In this model, the newly added node directly links to m_r nodes, while also making m_s preferential linking to some neighbors of m_r preferentially attached nodes to create triads. This significantly increases the GCC in CSF networks with the same average node degree as SF networks.

4.1. Empirical results and simulation

To study the effect of GCC, we compare the number/average-size of contractions in CSF/SF graphs. We perform Monte-Carlo simulations over 50 realizations of sample CSF and SF graphs with $m = m_r + m_s = 2$ and $n = 100$ to $n = 1000$ nodes. Having $m = m_r + m_s$ ensures equal number of new edges via preferential attachment in both CSF and SF networks, implying the same average node degrees for both types. This is essential for comparison as all features of both CSF and SF graphs must be similar while only their GCC differs [23]. Fig. 1 shows the Monte-Carlo simulation results.

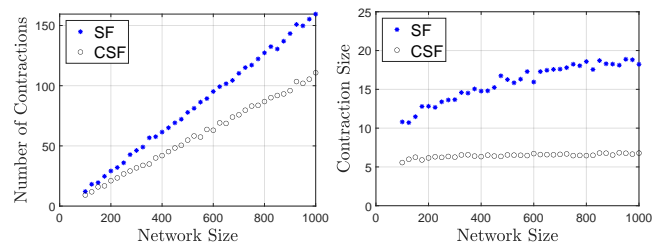


Fig. 1: Number and size of contractions averaged over 50 realizations of growing SF and CSF networks.

As shown in Fig. 1, in SF graphs there are more contractions which are in average larger (in size) as compared to CSF graphs. Table 1 summarizes the results shown in Fig. 1.

Table 1: Comparison of CSF and SF graph samples.

Graph Type	SF	CSF
Average size of Contraction	15.8	6.6
Average number of Contractions	86	59
Average GCC	0.017	0.181

¹GCC is defined as the ratio of the triangles tr to the total number of connected open triplets trp in the graph, i.e., $GCC = \frac{3 \cdot tr}{trp}$ [15].

4.2. Discussions on the results

From Fig. 1 and Table 1, we see the average size of contractions in SF networks is significantly larger than CSF networks. Recall that both graph types are constructed via the preferential attachment method and, therefore, both share similarity of most graph properties, e.g., (i) logarithmic growth in mean shortest-path and (ii) power-law degree distribution [23]. Their main difference stems from the GCC, which is lower in SF graphs. This is the key feature contributing to the decrease in both size and number of contractions in CSF graphs. Again we emphasize that the other graph properties of both types are similar. Thus, one can conclude that, in graphs with power-law degree distribution, increase in GCC causes fewer contractions with smaller average-size.

In terms of system observability/estimation, the implication is that for graphs with higher GCC: (i) fewer state measurements are needed to ensure observability; and (ii) fewer observationally equivalent states are available to recover observability loss in case of measurement failure. The first result deduced from number of contractions while the latter stems from average size of contractions. This implies that the observability (and consequently estimation properties) can be improved/deteriorated by tuning the GCC of (synthetic) system networks via [1, 16, 17]. A such example is given next.

5. ILLUSTRATIVE EXAMPLE: APPLICATION TO POWER NETWORKS

The power grid, as an engineered infrastructural network, can be conceived as a large-scale dynamical system [26], where the sparsity of its (linearized) system matrix follows the structure of the power distribution network [27]. To ensure reliable power delivery, the electrical phasor state (voltage, current, etc.) is typically measured via advanced sensors, known as phasor measurement units (PMUs), distributed over the electricity grid. The PMU placement is such that to ensure observability of the entire power grid for monitoring puposes [28]. Following the results of this paper, one can reduce the number of allocated PMUs for observability by changing the structure of the power network. Consider the European power grid [29] shown in Fig. 2(top) with 1494 nodes (buses) and 2156 edges (transmission lines). The unmatched nodes represent the possible location of PMU placement in the grid. Following the results in Section 4, we increase the GCC by adding 40 edges between certain bus-nodes in the network as shown in Fig. 2(bottom). The network grid properties before and after link addition are compared in Table 2. Note that the change in average node degree is negligible while the GCC is increased about 19%. As expected, contractions and unmatched nodes are reduced by 47% by adding only 40 edges which are about 1.8% of the total edges in the network.

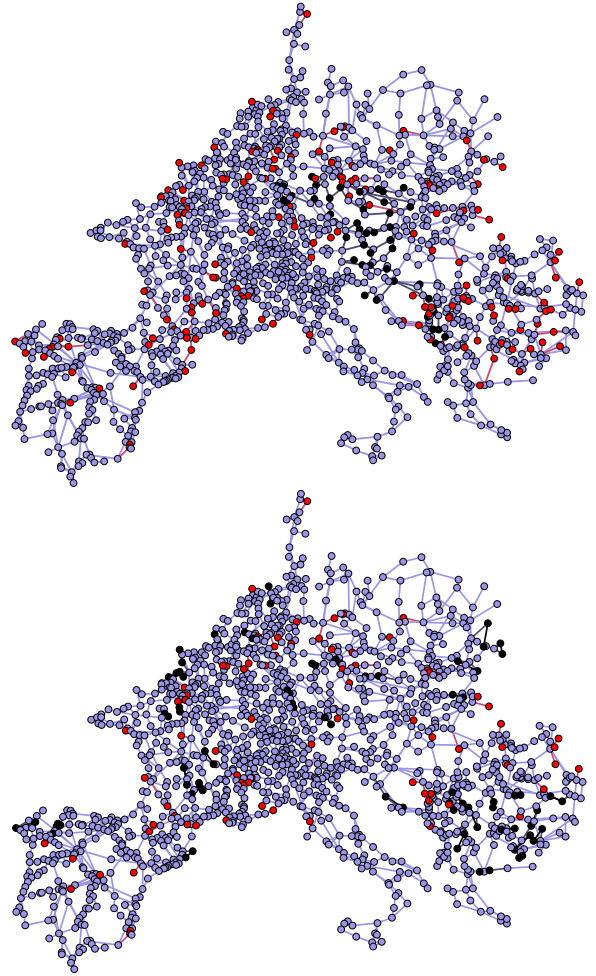


Fig. 2: (top) The European power grid with 151 unmatched bus-nodes (shown in red) whose states need to be measured via PMUs. An example contraction of 46 nodes is also shown in black. (bottom) By adding 40 edges (shown in black) to increase the GCC of power network, the number of unmatched bus-nodes (and minimum required PMUs) is reduced to 80.

Table 2: Network characteristics before/after link addition.

links	average degree	GCC	contractions
2156	2.886	0.094	151
2196	2.939	0.112	80

6. CONCLUSIONS AND FUTURE RESEARCH

In this work, distribution of contractions in SC digraphs and its relation with graph GCC is studied. Note that for general non-SC digraphs, another component known as *root SCC* or *parent SCC* also affects system graph observability [30, 31]. As future research, we intend to study the correlation between prevalence/size of both parent SCCs and contractions with other graph features, such as assortativity/disassortativity and community/hierarchical structure [15].

7. REFERENCES

- [1] M. Doostmohammadian and H. R. Rabiee, "On the observability and controllability of large-scale iot networks: Reducing number of unmatched nodes via link addition," *IEEE Control Systems Letters*, vol. 5, no. 5, pp. 1747–1752, 2020.
- [2] M. Rana, L. Li, and S. W. Su, "Distributed state estimation over unreliable communication networks with an application to smart grids," *IEEE Transactions on Green Communications and Networking*, vol. 1, no. 1, pp. 89–96, 2017.
- [3] H. Arasteh, V. Hosseinneshad, V. Loia, A. Tommasetti, O. Troisi, M. Shafie-khah, and P. Siano, "Iot-based smart cities: A survey," in *IEEE 16th International Conference on Environment and Electrical Engineering*. IEEE, 2016, pp. 1–6.
- [4] M. Doostmohammadian, H. R. Rabiee, H. Zarrabi, and U. A. Khan, "Distributed estimation recovery under sensor failure," *IEEE Signal Processing Letters*, vol. 24, no. 10, pp. 1532–1536, 2017.
- [5] M. Kabiri, N. Amjady, M. Shafie-khah, and J. P. S. Catalao, "Enhancing power system state estimation by incorporating equality constraints of voltage dependent loads and zero injections," *International Journal of Electrical Power & Energy Systems*, vol. 99, pp. 659–671, 2018.
- [6] J. M. Dion, C. Commault, and J. van der Woude, "Generic properties and control of linear structured systems: A survey," *Automatica*, vol. 39, pp. 1125–1144, Mar. 2003.
- [7] Y. Y. Liu, J. J. Slotine, and A. L. Barabási, "Controllability of complex networks," *Nature*, vol. 473, no. 7346, pp. 167–173, May 2011.
- [8] A. Ortega, P. Frossard, J. Kovačević, J. M. F. Moura, and P. Vandergheynst, "Graph signal processing: Overview, challenges, and applications," *Proceedings of the IEEE*, vol. 106, no. 5, pp. 808–828, 2018.
- [9] J. F. Carvalho, S. Pequito, A. P. Aguiar, S. Kar, and K. H. Johansson, "Composability and controllability of structural linear time-invariant systems: Distributed verification," *Automatica*, vol. 78, pp. 123–134, 2017.
- [10] M. Doostmohammadian, H. R. Rabiee, H. Zarrabi, and U. A. Khan, "Observational equivalence in system estimation: Contractions in complex networks," *IEEE Transactions on Network Science and Engineering*, vol. 5, no. 3, pp. 212–224, 2017.
- [11] C. Commault, J. Dion, D. H. Trinh, and T. H. Do, "Sensor classification for the fault detection and isolation, a structural approach," *International Journal of Adaptive Control and Signal Processing*, vol. 25, no. 1, pp. 1–17, 2011.
- [12] B. Guo, O. Karaca, T. H. Summers, and M. Kamgarpour, "Actuator placement under structural controllability using forward and reverse greedy algorithms," *IEEE Transactions on Automatic Control*, 2020.
- [13] S. Moothedath, P. Chaporkar, and M. N. Belur, "Minimum cost feedback selection for arbitrary pole placement in structured systems," *IEEE Transactions on Automatic Control*, vol. 63, no. 11, pp. 3881–3888, 2018.
- [14] M. Doostmohammadian, H. R. Rabiee, and U. A. Khan, "Structural cost-optimal design of sensor networks for distributed estimation," *IEEE Signal Processing Letters*, vol. 25, no. 6, pp. 793–797, 2018.
- [15] M. Newman, A. Barabási, and D. J. Watts, *The structure and dynamics of networks.*, Princeton university press, 2006.
- [16] N. Islam, "Towards a secure and energy efficient wireless sensor network using blockchain and a novel clustering approach," M.S. thesis, Dalhousie University, 2018.
- [17] J. M. Moore, M. Small, and G. Yan, "Inclusivity enhances robustness and efficiency of social networks," *Physica A: Statistical Mechanics and its Applications*, vol. 563, pp. 125490, 2021.
- [18] E. Montijano, G. Oliva, and A. Gasparri, "Distributed estimation and control of node centrality in undirected asymmetric networks," *IEEE Transactions on Automatic Control*, 2020.
- [19] M. Doostmohammadian, H. R. Rabiee, and U. A. Khan, "Cyber-social systems: modeling, inference, and optimal design," *IEEE Systems Journal*, vol. 14, no. 1, pp. 73–83, 2019.
- [20] J. Lovato, A. Allard, R. Harp, and L. Hébert-Dufresne, "Distributed consent and its impact on privacy and observability in social networks," *arXiv preprint arXiv:2006.16140*, 2020.
- [21] K. Murota, *Matrices and matroids for systems analysis*, Springer, 2000.
- [22] M. Doostmohammadian and U. A. Khan, "On the distributed estimation of rank-deficient dynamical systems: A generic approach," in *IEEE International Conference on Acoustics, Speech and Signal Processing*. IEEE, 2013, pp. 4618–4622.
- [23] P. Holme and B. J. Kim, "Growing scale-free networks with tunable clustering," *Physical review E*, vol. 65, no. 2, pp. 026107, 2002.
- [24] I. Türker, "Generating clustered scale-free networks using poisson based localization of edges," *Physica A: Statistical Mechanics and its Applications*, vol. 497, pp. 72–85, 2018.
- [25] C. P. Herrero, "Ising model in clustered scale-free networks," *Physical Review E*, vol. 91, no. 5, pp. 052812, 2015.
- [26] J. Machowski, Z. Lubosny, J. W. Bialek, and J. R. Bumby, *Power system dynamics: stability and control*, John Wiley & Sons, 2020.
- [27] U. A. Khan and M. Doostmohammadian, "A sensor placement and network design paradigm for future smart grids," in *4th International Workshop on Computational Advances in Multi-Sensor Adaptive Processing*, Puerto Rico, 2011, pp. 137–140.
- [28] R. Babu and B. Bhattacharyya, "Optimal allocation of phasor measurement unit for full observability of the connected power network," *International Journal of Electrical Power & Energy Systems*, vol. 79, pp. 89–97, 2016.
- [29] "The RE-Europe data set," <https://zenodo.org/record/35177>.
- [30] S. Pequito, V. M. Preciado, A. Barabási, and G. J. Pappas, "Trade-offs between driving nodes and time-to-control in complex networks," *Scientific reports*, vol. 7, no. 1, pp. 1–14, 2017.

- [31] M. Doostmohammadian and U. A. Khan, "On the characterization of distributed observability from first principles," in *2nd IEEE Global Conference on Signal and Information Processing*, 2014, pp. 914–917.